

Latex Film Formation and Dissolution: A Fluorescence Study

Önder Pekcan* and Şaziye Uğur

Istanbul Technical University, Department of Physics, 80626, Maslak,
Istanbul, Turkey

Abstract: A new technique based on steady state fluorescence (SSF) measurements is introduced for studying dissolution of polymer films. These films are formed from naphthalene (N) and pyrene (P) labeled poly(methyl methacrylate) (PMMA) latex particles, sterically stabilized by polyisobutylene (PIB). Annealing was performed above T_g at elevated temperatures for 30 min time intervals for film formation. Film formation from these latexes is monitored by the extent of energy transfer from N to P using SSF and by the transmitted photon intensity from these films using UV visible (UVV) methods. Desorption of P labeled PMMA chains was monitored in real-time by the change of pyrene fluorescence intensity. Dissolution experiments were performed in various solvents with different solubility parameters, δ , at room temperature. Diffusion coefficients, D , in various solvents were measured and found to be around 10^{-10} cm²/s. Strong relationships between D and δ were observed. Diffusion activation energy was measured by performing dissolution experiments in toluene-heptane mixtures at elevated temperatures and determined to be 24.4 kcal mol⁻¹.

INTRODUCTION

Film formation from latexes is a complicated, multi-stage phenomenon and depends strongly on the characteristics of colloidal particles. In general, aqueous or non-aqueous dispersion of colloidal particles with a glass transition temperature (T_g) above the drying temperature are named hard latex dispersions. An aqueous dispersion of colloidal particles with a T_g below the drying temperature is called soft latex dispersion. The term "latex film" normally refers to a film formed from soft particles, in which the forces accompanying the evaporation of water are sufficient to compress and deform the particles into a transparent, void-free film^{1,2}. However, hard latex particles remain essentially discrete and undeformed during the drying process. Film formation from these dispersion can occur in several stages. In both cases, the first stage corresponds to the initial wet stage. Evaporation of solvent leads to a second stage in which the particles form a closed packed array. Here, if the particles are soft, they are deformed to polyhedrons. Hard latex particles however stay

undeformed at this stage. Annealing of soft particles causes diffusion across particle-particle boundaries, which leads to a homogeneous continuous film material. In the annealing of hard latex systems however, deformation of particles first leads to void closure^{3),4)} and then, after the voids disappear, diffusion across particle-particle boundaries begins, i. e. the mechanical properties of hard latex films can be developed by annealing; after all solvent has evaporated and all the voids have disappeared.

Polymer films obtained from latex particles are usually used for their resistance to permeation by organic solvents, water, oxygen and other corrosive agents. Consequently, dissolution of polymers in organic solvents has attracted attention for the photoresist dissolution process in integration circuits⁵⁻⁷⁾. In controlled release applications of polymers a solute is dispersed or molecularly dissolved in a polymer phase⁸⁾. The release process can be controlled either by solvent diffusion or by polymer dissolution.

Poly methyl methacrylate (PMMA) film dissolution was first studied using laser interferometry by varying molecular weight and solvent quality⁹⁾. Winnik and coworkers modified the interferometric technique and studied the dissolution of fluorescence labeled PMMA films¹⁰⁾ by monitoring the intensity of fluorescence from the film together with the interferometric signal. The solvent penetration rate into the film and the film dissolution were measured simultaneously. Fluorescence quenching and depolarization methods have been used for penetration and dissolution studies in solid polymers¹¹⁻¹³⁾. The real-time, nondestructive method for monitoring small molecule diffusion in polymer films has been developed¹⁴⁻¹⁷⁾. This method is based on the detection of excited fluorescence dyes desorbing from a polymer film into a solution in which the film has been placed. Recently, we have reported a steady state fluorescence (SSF) study on dissolution of both annealed latex film¹⁸⁾ and PMMA discs using real-time monitoring of fluorescence probes^{19),20)}.

The mechanism of polymer film dissolution is much more complicated than small molecule dissolution. Small molecule dissolution can be explained by Fick's law of diffusion with a unique diffusion rate²¹⁾. However, in polymeric systems many anomalies or deviations from Fick's law of diffusion are observed²²⁾, particularly below the glass transition temperature of a polymer. In general this question of non-Fickian or anomalous diffusion can be perhaps subdivided into two sub-

questions. The first concerns sorption of solvent into the glassy polymers. The second deals with desorption of solvents from swollen polymers. The most characteristic feature of the former is that the amount of solvent sorbed into the polymer varies with time raised to an exponent between 0.5 and 1.0, where the extreme case (1.0) is called Case II diffusion. The final step of polymer dissolution is called mutual diffusion of the polymer and solvent molecules in liquid phase.

In this work latex film samples were prepared from dispersion of N and P labeled PMMA particles. Various solvents with different solubility parameters were used as dissolution agents. In-situ, SSF experiments were performed by real-time monitoring of dissolution processes. Dissolution experiments were performed in solvents at room temperature. Dissolution experiments were designed so that P labeled PMMA chains, desorbing from swollen gel were detected by the SSF method. To achieve this direct illumination of the film sample is avoided, during the in-situ dissolution experiment. Our main goal in the work presented here is to create mechanically strong latex films by annealing, and then study the dissolution process in various solvents to determine the relation between diffusion (D) and solubility (δ) parameters. In another set of experiments, films are dissolved in toluene-heptane mixture at temperatures between 25-65 °C. Here the goal was to slow down the solubility by adding heptane into the system. The dissolution temperature was then increased to determine the dissolution activation energy.

THEORETICAL CONSIDERATION

Various mechanisms and various mathematical models have been considered for polymer dissolution. Quano²³⁾ proposed a model which includes polymer diffusion in a liquid layer adjacent to the polymer and moving of the liquid-polymer boundary. The key parameter for this model is the polymer disassociation rate, defined as the rate at which polymer chains desorb from the gel interface. Peppas²⁴⁾ extended this model for films to include situations of polymer dissolution rate for which gel thickness was found to be proportional to $(\text{time})^{1/2}$. A relaxation controlled model was proposed by de Gennes and Brochard²⁵⁾ where, after a swelling gel layer was formed, desorption of polymer from the swollen bulk was governed by the relaxation rate of the polymer stress. This rate was found to be of the same order of magnitude as the reptation time. The dependencies of the radius of gyration and the reptation time on polymer molecular weight and concentration were studied, using a scaling law²⁶⁾ based on the reptation model.

In this paper, we have employed a simpler model developed by Enscoe et.al.²⁷⁾ to interpret the results of polymer swelling and dissolution experiments. This model includes Case I and Case II diffusion kinetics.

Case I or Fickian Diffusion

The solution of a unidirectional diffusion equation for a set of boundary conditions is cited by Crank^{21),22)}. For a constant diffusion coefficient, D , and fixed boundary conditions, the sorption and desorption transport in and out of a thin slab is given by the following relation

$$\frac{M_t}{M_\infty} = 1 - \frac{8}{\pi^2} \sum_{n=0}^{\infty} \frac{1}{(2n+1)^2} \exp\left(-\frac{(2n+1)^2 D \pi^2 t}{d^2}\right) \quad (1)$$

Here, M_t represents the amount of materials absorbed or desorbed at time t , M_∞ is the equilibrium amount of material, and d is the thickness of the slab.

Case II Diffusion

Case II Transport mechanism is characterized by the following steps. As the solvent molecules enter into the polymer film, a sharp advancing boundary forms and separates the glassy part of the film from the swollen gel (see Fig 1b). This boundary moves into the film at a constant velocity. The swollen gel behind the advancing front is always at a uniform state of swelling. Now, consider a cross-section of a film with thickness d , undergoing Case II diffusion as in (Fig. 1), where L is the position of the advancing sorption front, C_0 is the equilibrium penetrant concentration and k_0 ($\text{mg}/\text{cm}^2 \text{ min}$) is defined as the Case II relaxation constant. The kinetic expression for the sorption in the film slab of an area A is given by

$$\frac{dM_t}{dt} = k_0 A \quad (2)$$

The amount of penetrant, M_t absorbed in time t will be

EXPERIMENTAL

Naphthalene (N) and pyrene (P)-labeled PMMA-PIB latex particles were prepared separately by a two-step process. In the first step, MMA was polymerized to low conversion in cyclohexane in the presence of PIB containing 2% isoprene units to promote grafting. The graft copolymer produced served as a dispersant in the second stage of polymerization, in which MMA was polymerized in a cyclohexane solution of copolymer. Details have been published²⁸⁾ elsewhere. A stable spherical high-T dispersion of polymer particles was produced, ranging in radius from 1 to 3 μm . A combination of ^1H -NMR and UV analysis indicated that these particles contained 6 mol % PIB and 0.37 mmol N and 0.037 mmol P groups per gram of polymer. We refer to these particles as N and P respectively. (These particles were prepared in M. A. Winnik's Lab in Toronto)

Latex film preparations were carried out in the manner following: the same weights of N and P particles were dispersed in heptane in a test tube for which the solid content was 0.24 %. Film samples were prepared from this dispersion, by placing various number of drops on $3 \times 0.8 \text{ cm}^2$ glass plates and allowing the heptane to evaporate. Here, we were careful that the liquid dispersion from the droplets covered the whole surface area of the plate and remained there until the heptane had evaporated. Samples were weighed before and after the film casting to determine the film thickness. The average film thickness was estimated to be ca. 12 μm . Average size for the particles was taken as 2 μm to estimate the number of layers or the thickness of the film samples. The films were annealed for 30 min time interval above the T_g of PMMA at elevating temperatures up to 210 $^{\circ}\text{C}$ in an oven. The temperature was maintained within $\pm 2^{\circ}\text{C}$ during annealing.

UV visible experiments were carried out with the model Lambda 2S UV-Visible spectrometer of Perkin Elmer. The transmittance of latex films were measured between 300-400 nm.

For the dissolution experiments, various solvents were chosen with different solubility parameters. Spectroscopically pure grade Ethyl Benzene (EB), Toluene (TO), Ethyl Acetate (EA), Benzene (BE), Chloroform (CH), Dichlorometan (DM), Tetrahydrofuran (THF) and Acetone (AC) were purchased from Merck Co. and used as received.

Dissolution experiments were performed in a 1.0x1.0 cm quartz cell. This cell was placed in the spectrofluorimeter and fluorescence emission was monitored at 90° angle so that film samples were not illuminated by the excitation light. Film samples were attached to one side of the quartz cell filled with solvent. The cell was then illuminated with 345 nm excitation light. Pyrene fluorescence intensity, I_p , was monitored during the dissolution process at 375 nm using the "time drive" mode of spectrofluorimeter. Emission of P-labeled polymer chains was recorded continuously at 375 nm as a function of time until there was no observable change in intensity. The dissolution cell and the film position is presented in (Fig. 2). Eight different dissolution experiments were run for the given solvents. In the other set of experiments toluene (80 %) and heptane (20 %) mixture was used for the dissolution and samples were kept at 25, 30, 35, 40, 45, 50, 55, 60 and 65 °C temperatures during dissolution processes. Solvent were purchased from Merck Co. (spectroscopically pure grade) and used as received. Since toluene is good solvent for PMMA, heptane was introduced into the mixtures to slow down the dissolution process in the second set of experiments.

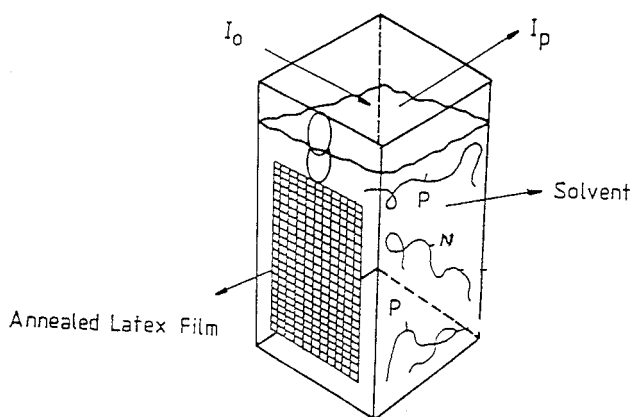


Fig. 2 Dissolution cell in LS-50 Perkin Elmer Spectrophotometer. I_0 and I_p are the exciting and emitted light intensities at 345 nm and 375 nm, respectively.

RESULTS AND DISCUSSION

Latex Film Formation

Typical fluorescence emission spectra of N-P films, when excited at 286 nm are shown in (Fig. 3a) and b, before and after annealing at 130, 150, 190 °C respectively. As the annealing temperature is

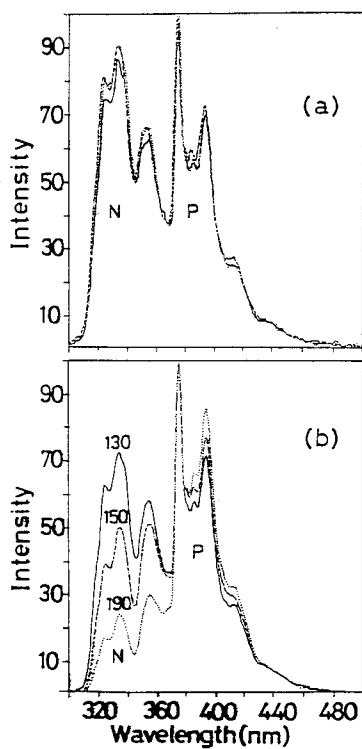


Fig. 3 Emission spectra of Naphthalene (N) and Pyrene (P) when latex film samples are excited at 286 nm a- Before annealing, b- After annealing at 130, 150 and 190 °C for 30 min.

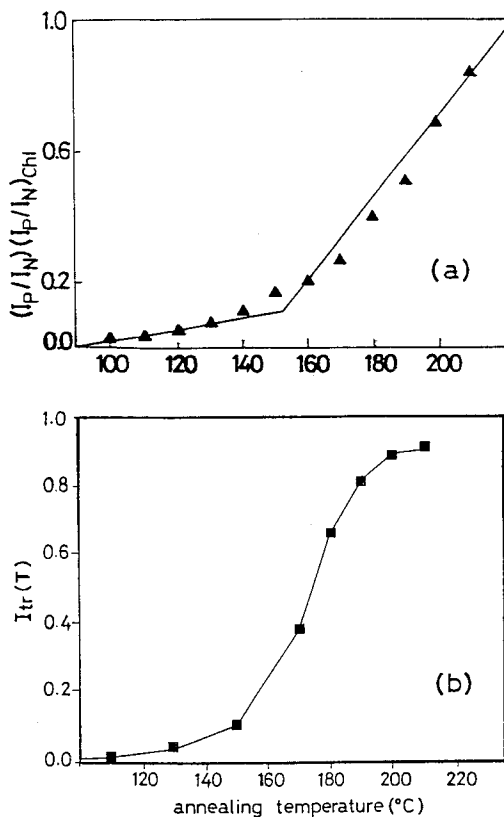


Fig. 4 a- plot of $(I_P/I_N)/(I_P/I_N)_{\text{Chl}}$ versus annealing temperature. $(I_P/I_N)_{\text{Chl}}$ ratio from the chloroform (Chl) cast film is used to obtain normalized intensity ratios. b- Plot of transmitted light intensity versus annealing temperatures.

increased N intensity, I_N , decreases and P intensity, I_P , increases, indicating that energy transfer from N to P takes place. In order to show the evolution of energy transfer from N to P, normalized (I_P/I_N) ratios were plotted versus annealing temperature (Fig. 4a). Here, the chloroform cast film is used to obtain normalized intensity ratios¹⁸⁾, where N-P mixing for energy transfer is almost 90 %. It is seen that above 150 °C energy transfer increases dramatically. Fig. 4b presents the plot of the transmitted

light intensity, I_{tr} , from the latex film versus annealing temperature. A sudden increase in I_{tr} is observed at 150 °C, and 90 % transparency was reached by annealing the film at 200 °C. These observations are in general agreement with the fluorescence data.

Film Dissolution

During in-situ dissolution experiments P labeled polymer chains were excited at 345 nm and the variation in fluorescence emission intensity, I_p , was monitored with the "time drive" mode of spectrofluorimeter. (Fig. 5) presents the P intensities, I_p , as a function of "dissolution time" for film samples dissolved in various solvents. These curves reach a plateau in an almost similar fashion at long times except for that of EB. Curves for CH and DM reach a plateau very quickly indicating fast dissolution of films. Dissolution curves for TO, EA, BE, THF and AC are much slower than the CH and DM curves. The curve for EB seems to reach a plateau at very long times, i.e. dissolution obeys a different diffusion model.

The dissolution curves, in (Fig. 5) can be quantified by fitting the data to Eq 1. Figs. 6a, b and c present plots of the following relation, for film samples dissolved in TO, AC and DM, respectively.

$$\ln\left(1 - \frac{I_p}{I_{p\infty}}\right) = B - At \quad (7)$$

This is the logarithmic form of Eq 1 for $n=0$ with $A=D\pi^2/d^2$ and $B=\ln(8/\pi^2)$. Here, it is assumed that I_p is proportional to the number of P labeled chains desorbing from the latex film and $I_{p\infty}$ represents its value at the equilibrium condition. It has to be mentioned that the swelling process for the polymer film was too fast to be observed¹⁸⁻²⁰⁾ for all solvents except for EB, which has a very low solubility parameter and shows complete Case II diffusion behavior. In Fig. 6 all the dissolution curves were digitized for the numerical treatment. When the curves in Figs. 6a, b and c are compared with computations using Eq 7, chain desorption coefficients, D , are obtained. The linear fit of Eq 7 to the data produces D values. D values for the films dissolved in CH and DM are found to be much larger than the other solvents. When one compares the observed $D \approx 10^{-10}$ cm²/sec values with the

backbone diffusion coefficient of interdiffusing polymer chains during film formation from PMMA latex particles^{29,30}), ($\approx 10^{-16}$ - 10^{-14} cm²/sec), 6 to 4 orders of magnitude difference can be seen.

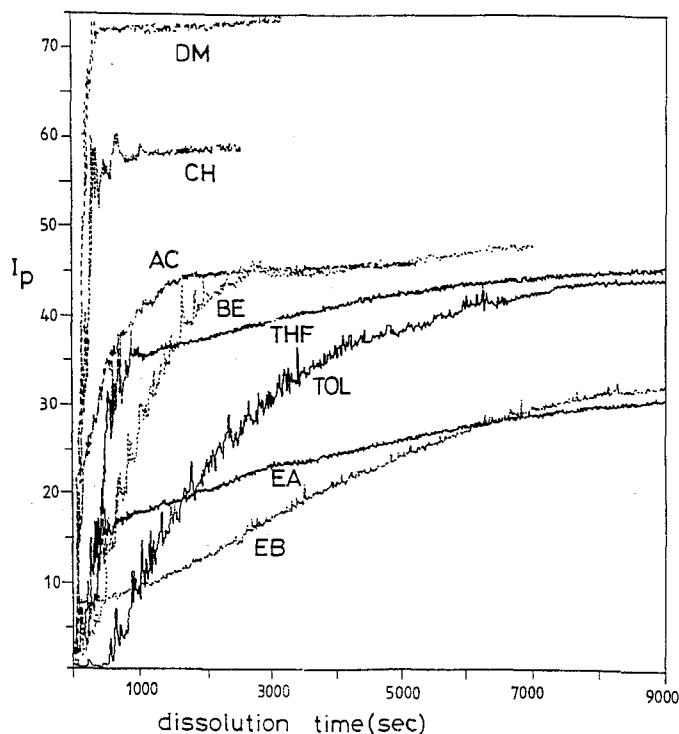


Fig. 5 Pyrene intensity, I_p , versus dissolution time for the film samples dissolved in various solvents. The cell was illuminated at 345 nm during fluorescence measurements. Data for the plot were obtained using the time drive mode of the spectrofluorimeter.

This is reasonable for the chains desorbing from swollen gel, during dissolution of PMMA latex films. In fact, 10^{-10} cm²/sec is two orders of magnitude smaller than the D values obtained for oxygen diffusing into PMMA spheres³¹). This may suggest that penetration of solvent molecules into a latex

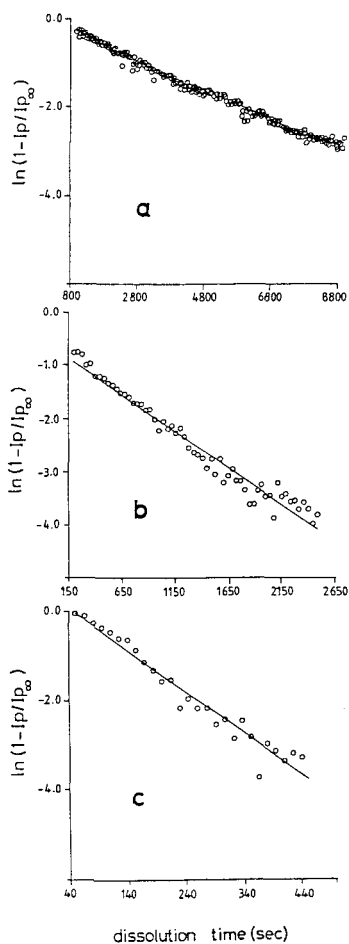


Fig. 6 Comparison of the data at linear time region presented in Fig. 5 with the computations using equation 7. Desorption coefficients, D , are obtained from the slopes of the plots in a, b and c for the films dissolved in TO, AC and DM respectively.

film is almost as fast as desorption of PMMA chains from a swollen gel. Here, one should realize that solvent molecules are much larger in size than oxygen molecules. Our D values (10^{-10} cm²/sec)

are also similar to the D values (10^{-11} cm²/sec) obtained for n-hexane desorption from polystyrene spheres³².

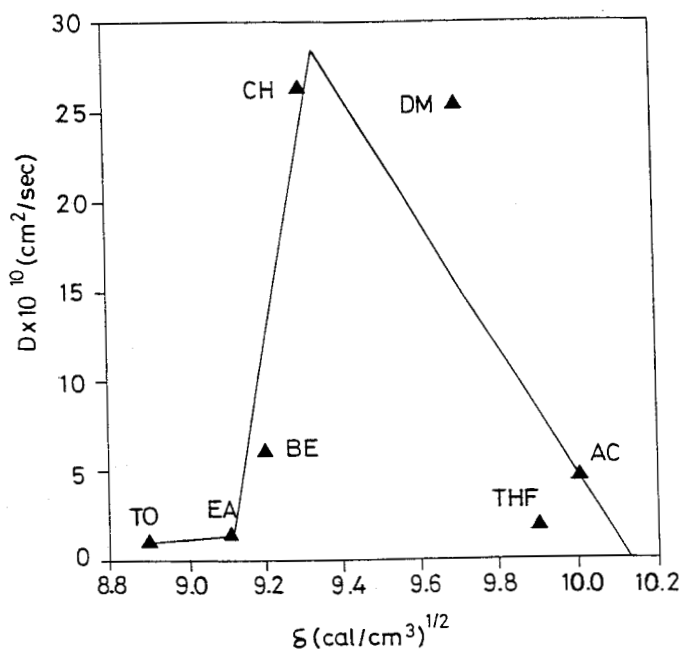


Fig. 7 Plot of D versus solubility parameter δ of solvents.

It is important to note that diffusion of solvent molecules into the latex film depends substantially upon the hydrocarbon employed. The challenge is to figure out whether kinetic effects associated with the solvent viscosity (η) or thermodynamic effect (polymer-solvent interaction) are responsible for the dissolution of the latex film. No correlation has been found between η and D values. Here it is convenient to test whether the solvent quality i.e. polymer-solvent interactions are responsible or not for the dissolution processes. Solution theory predicts that the polymer-solvent interaction

parameter is related to the solubility parameter (δ) and the molar volume (V) via the following relation³³⁾

$$\chi = \frac{V}{RT}(\delta - \delta_p)^2 \quad (8)$$

Where R is the gas constant, T is the temperature and δ_p is the solubility parameter of the polymer. This theory leads to the conclusion that polymers dissolve in small molecular liquids only if $(\delta - \delta_p)$ is very small. A plot of D versus δ in (Fig. 7) shows that there is a strong correlation between χ and D values i.e. as $(\delta - \delta_p)$ approaches zero, D values are very large (where $\delta_p = 9.3 \text{ (cal/cm}^3)^{1/2}$ was taken for PMMA). Here, larger D value for DM molecules most probably result from the smaller molar volume of this molecule. From this one can conclude that the chain desorption (diffusion) coefficient is strongly correlated to the polymer-solvent interaction parameter(χ).

Here, a basic conclusion can be deduced that the desorption (i.e. diffusion) coefficient, D , is strictly a thermodynamic quantity, which mostly associates with the solubility parameter during latex film dissolution. In other words, the rate limiting step during polymer film dissolution is the polymer-solvent interaction, which may strongly affect the chain desorption from the swollen gel.

Diffusion Activation Energies

Fig. 8 presents I_p versus dissolution time for film samples dissolved in toluene-heptane mixture at various temperatures. All the curves reached a plateau except that for 25°C . Temperature dependence of D values can be interpreted by assuming that Case I diffusion obeys the Arrhenius relation as follow

$$D = D' \exp\left(-\frac{\Delta E_D}{kT}\right) \quad (9)$$

here, k is the Boltzmann constant, D' is the preexponential factor, and ΔE_D is the activation energy of Case I diffusion, respectively.

Dissolution curves in Fig. 8 of this set of experiments were digitized for mathematical treatment according to Eq (7) and the results are plotted in Fig. 9. The curve for the sample dissolved at 25 °C shows pure Case II behavior. However, curves in Fig. 9b and c show Case I characteristics. If we assume that the amount of the penetrant is proportional to the number of PMMA chains desorbing from the

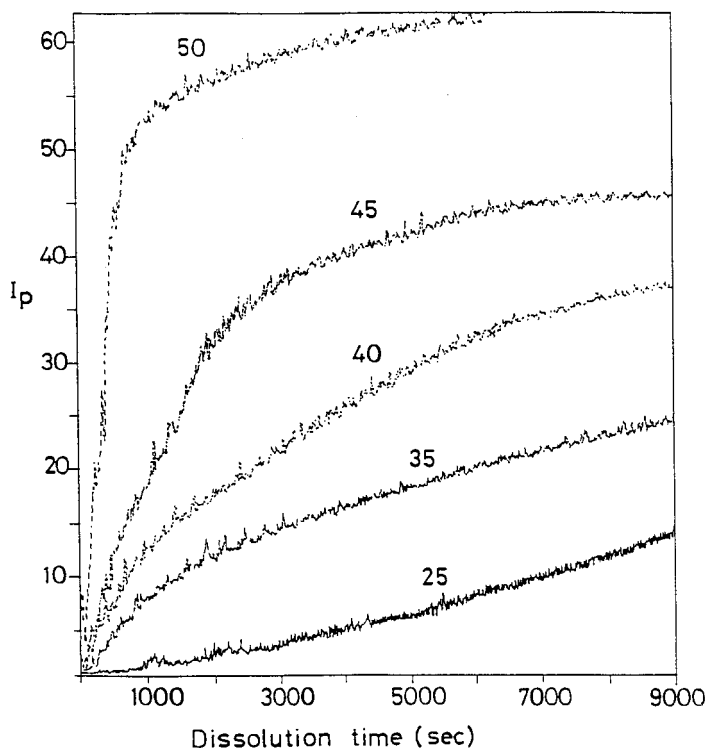


Fig. 8 Pyrene intensity, I_p , versus dissolution time for the film samples dissolved at 25 °C, 35 °C, 45 °C and 50 °C in toluene (80 %)-heptane (20%) mixtures.

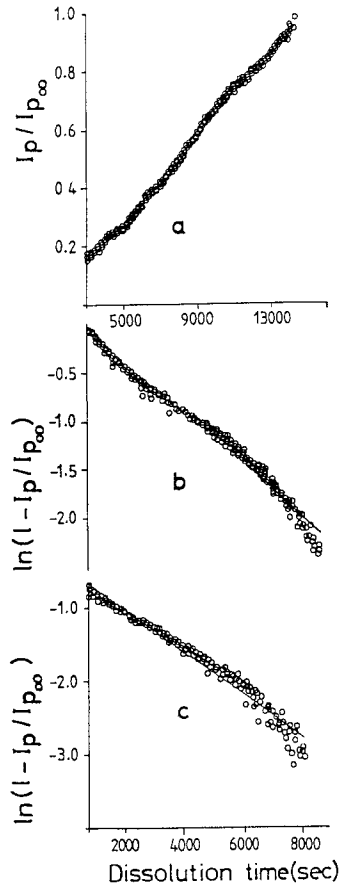


Fig. 9 Comparison of the linear portions of the data presented in (Fig. 8) with the computation for a using equation 10, b and c using equation 7. Relaxation (k_0) and diffusion constants (D) are obtained from the slopes of the plots in a and b, c for the films dissolved at 25 °C and 35 °C, 45 °C respectively.

swollen gel than Eq 6 can be written as

$$\frac{I_p}{I_\infty} = \frac{k_0}{C_0 d} t \quad (10)$$

k_0 may be obtained from Eq 10 and the slope of the graph in (Fig. 9a). Here, $C_0=0.86$ g/ml and d value listed in Table I is used. Data in (Fig. 9b and c) are fit to Eq (7) to produce D values. Experimentally obtained D and k_0 values are given in Table I; k_0 values for high temperatures are missing.

Table I: Experimentally obtained diffusion (D) and relaxation (k_0) parameters during dissolution of latex films in (toluene-heptane) mixtures at various temperatures.

T ($^{\circ}\text{C}$)	$dx10^{-4}$ (cm)	$Dx10^{-11}$ (cm^2/sec)	k_0x10^{-2} ($\text{mg}/\text{cm}^2\text{min}$)
25	11.2	-	0.412
30	9.05	-	0.378
35	10.5	2.4	-
40	9.66	2.26	-
45	9.24	2.92	-
50	9.24	4.53	-
55	10.08	7.9	-
60	10.76	26.5	-
65	9.24	32.4	-

Using Table I and Eq (9), diffusion activation energy ΔE_D was calculated and found to be 24.41 kcal/mol. Arrhenius plot for D is presented in (Fig. 10). The ΔE_D value obtained from the experiment is quite close to the energy characteristic of a polymer chain backbone motion^{34),35)}. From this we can conclude that during dissolution processes, after creation of a gel layer, polymer chains disentangle, with the help of their side chain motion, and then diffuse into the solvent reservoir by their translational backbone motion.

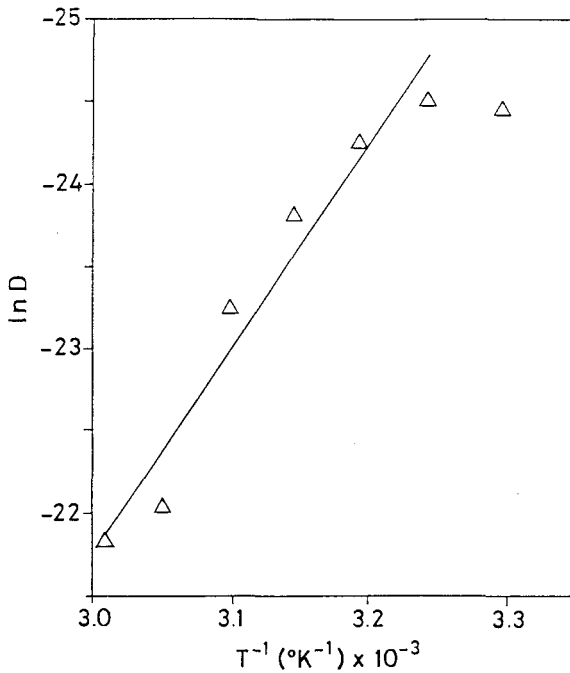


Fig. 10 Plot of the logarithmic form of equation 9 for the data in Table I. $\Delta E_D = 24.4$ kcal/mol is obtained from the slope of the straight line.

REFERENCES

- ¹⁾ S. T. Eckersley and A. Rudin, *J. Coatings Technol.* 62, No. 780, 89 (1990).
- ²⁾ M. Joanicot, K. Wong, J. Maquet, Y. Chevalier, C. Pichot, C. Graillat, P. Linder, L. Rios and B. Cabane, *Prog. Coll. Polym. Sci.* 81, 175 (1990).
- ³⁾ P. R. Sperry, B. S. Snyder, M. L. O'Down and P. M. Lesko, *Langmuir*, 10, 2619 (1994).
- ⁴⁾ J. K. Mackenzie and R. Shuttleworth, *Proc. Phys. Soc.* 62, 838 (1946).
- ⁵⁾ A. C. Quano *Polym. Eng. Sci.* 18, 306 (1984).
- ⁶⁾ F. Rodriguez, P. D. Krasicky and R. J. Groele, *Solid State Tech.* May, p. 125 (1985).
- ⁷⁾ W. Limm, G. D. Dimnik, D. Stanton, M. A. Winnik and B. A. Smith, *J. Appl. Polym.*

- Sci., 35, 2099 (1988).
- ⁸⁾ P. Colombo, A. Gazzaniga, C. Caramella, U. Conte, A. L. Manna, *Acta, Pharm. Technol.* 33, 15 (1987).
 - ⁹⁾ P. D. Krasicky and R. J. Groele, F. Rodriquez, *J. App. Sci.* 35, 641 (1988).
 - ¹⁰⁾ W. Limm, G. D. Dimnik, D. Stanton, M. A. Winnik and B. Smith, *J. Appl. Polym. Sci.*, 35, 2099 (1988).
 - ¹¹⁾ J. E. Guilet in ‘‘Photophysical and Photochemical Tools in Polymer Science’’Ed. M. A. Winnik, Reidel, Dordrecht, 1986.
 - ¹²⁾ T. Nivaggioli, F. Wank, M. A. Winnik, *J. Phys. Chem.* 96, 7462 (1992).
 - ¹³⁾ D. Pascal, J., Duhamel, J. Wank, M. A. Winnik, Dh. Napper and R. Gilbert, *Polymer* 34, 1134 (1993).
 - ¹⁴⁾ L. Lu and R. G. Weiss, *Macromolecules*, 27 (1), 219, (1994).
 - ¹⁵⁾ V. V. Krongauz, W. F. Mooney III, J. W. Palmer, and J. J. Patricia, *J. Appl. Polym. Sci.* 56 (9), 1077 (1995).
 - ¹⁶⁾ V. V. Krongauz and R. M. Yohannan, *Polymer* 31 (9), 1130 (1990).
 - ¹⁷⁾ Z. He., G. S. Hammond, and R. G. Weiss, *Macromolecules*, 25 (1), 501 (1992).
 - ¹⁸⁾ Ö. Pekcan, M. Canpolat and D. Kaya, *J. App. Polymer Sci.* 60, 2105 (1996).
 - ¹⁹⁾ Ö. Pekcan, Ş. Uğur and Y. Yılmaz, *Polymer*, 38, 2183 (1997).
 - ²⁰⁾ Ş. Uğur and Ö. Pekcan, *Polymer*, 38, 5579 (1997).
 - ²¹⁾ J. Crank ‘‘The Mathematics of Diffusion’’, Clarendon Press, Oxford (1975).
 - ²²⁾ J. Crank and G. S. Park ‘‘Diffusion in Polymer’’, Acad. Press, London, 1968.
 - ²³⁾ Y. O. Tu and A. C. Quano *IBM J. Res. Dev.* 21, 131 (1977).
 - ²⁴⁾ P. I. Lee and N. A. Peppas *J. Controlled Release* 6, 207 (1987).
 - ²⁵⁾ F. Brochard and P. G. de Gennes *Physico. Chem. Hydrodynamics* 4, 313 (1983).
 - ²⁶⁾ J. S. Papanu, D. S. Soane and A. T. Bell. *J. Appl. Polym. Sci.* 38, 859 (1989).
 - ²⁷⁾ D. J. Ensco, H. B. Hopfenberg and V. T. Stannett *Polymer*, 18, 793 (1977).
 - ²⁸⁾ M. A. Winnik, M. H. Hua, B. Honhham, B. Williamson and M. D. Croucher, *Macromolecules* 17, 262 (1984).
 - ²⁹⁾ M. A. Winnik, Ö. Pekcan and M. D. Croucher, *Scientific Methods for the Study of Polymer Colloids and their App.* Ed. F. Candau and R. H. Ottewill. NATO, ASI 1988 Kluwer. Acad. Publish.

- ³⁰⁾ Ö. Pekcan, M. A. Winnik and M. D. Croucher, *Macromolecules* 23, 2673 (1990).
- ³¹⁾ Y. Kaptan, Ö. Pekcan and O. Güven, *J. App. Polym. Sci.* 44, 1595 (1992).
- ³²⁾ C. H. M. Jacques and H. B. Hopfenberg, *Polymer Eng. Sci.* 14, 449 (1974).
- ³³⁾ P. J. Flory, "Principles of Polymer Chemistry", Cornell University Press, Ithaca N. Y., 1953.
- ³⁴⁾ M. Canpolat and Ö. Pekcan, *Polymer* 36, 4433 (1995).
- ³⁵⁾ M. Shiotani and J. Sohma, *Polymer J.* 9, 283 (1977).